THE JOURNAL OF PHYSICAL CHEMISTRY Letters

Letter

pubs.acs.org/JPCL

Ionic Vapor: What Does It Consist Of?

Vitaly V. Chaban* and Oleg V. Prezhdo

Department of Chemistry, University of Rochester, Rochester, New York 14627, United States

Supporting Information

ABSTRACT: A comprehensive description of room-temperature ionic liquids (RTILs) requires characterization of their properties around normal boiling and critical. Using a thoroughly parametrized force field, we report atomistic simulations of the vapor phase of *N*-butylpyridinium tetrafluoroborate and 1-ethyl-3-methylimidazolium bis-(trifluoromethanesulphonyl)amide, existing in equilibrium with the liquid phase. We show that in contrast to traditional gases comprised of one type of molecules, the saturated vapor of RTILs consists of a broad range of structures, involving both neutral and charged species. While typically the ionic pair is the most stable vapor structure, the species distribution depends on RTIL chemical composition and is sensitive to temperature and pressure.

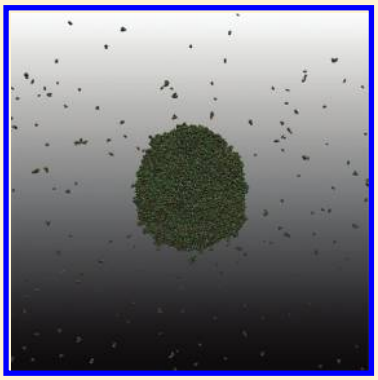

SECTION: Liquids; Chemical and Dynamical Processes in Solution

The field of room-temperature ionic liquids (RTILs) has witnessed an outstanding growth during the past decade.[1−6] More ionic species are synthesized, and new applications are constantly reported based on the numerous favorable properties of RTILs.[5−15] For a long time, RTILs were considered completely nonvolatile.[2,4] The experimental vapor pressures ranged between 0.01 and 1 Pa.[15,16] RTILs were viewed as nonflammable and thermally and chemically stable salts.[2] However, recently, certain aprotic RTILs were successfully distilled without degradation.[1,17,18] These works have highlighted the importance of understanding the physicochemical properties and atomistic organization of RTIL systems at elevated temperatures and, particularly, near the boiling point.

Poor thermal stability sometimes prevents direct experimental studies of high-temperature regions of RTILs, except at exceptionally low pressures.[19] Although most RTILs will decompose before reaching their critical, and sometimes boiling, points, such data are very important for creating and probing liquid-state models of these unusual compounds. The state of ions in the vapor phase remains controversial, as debated in recent works.[1,19−24] In particular, Earle et al. suggest that RTIL vapor is a collection of individual ions.[1] These results are generally supported by Ballone et al.,[25] who employ all-atom empirical potential models of interionic interactions. In contrast, recent publications suggest that vapor contains only neutral ion pairs.[17,20,22,26−29] There exist more exotic predictions, particularly, of stable neutral clusters involving several ion pairs.[25] In the meantime, interesting and conflicting experimental data have been reported regarding the variation of enthalpy and vapor pressure with the cation size and external conditions.[2,15,16,28,30−34] In experiment, even insignificant impurities can lead to great differences in measured vapor pressures and enthalpies, especially at very high temperatures. Therefore, it is highly desirable to provide a theoretical, atomistic-level description of RTIL vapor. This goal can be achieved by empirical force field (FF) models that have been thoroughly parametrized based on accurate ab initio computations.[35]

We report equilibrium and real-time nonequilibrium molecular dynamics (MD) simulations in order to gain insights into the boiling and critical behavior of *N*-butylpyridinium tetrafluoroborate ([BuPY][BF_4]) and 1-ethyl-3-methylimidazolium bis(trifluoromethanesulphonyl)amide ([EMIM][TFSA]). The analysis of ionic formations in the vapor phase is performed at 1000, 1050, 1075, and 1100 K, which are below the normal boiling point, T_b, of the respective RTILs. While below T_b, these temperatures are sufficient to produce significant saturated vapor pressures.

We implement the liquid/vapor interface explicitly by elongating the simulation cell along one of the Cartesian directions. The resulting periodic system can be imagined as a thin RTIL film surrounded by a large slab of vacuum. The vacuum will be filled with RTIL vapor upon heating. Figure 1 summarizes total nonbonded potential energies, saturated pressures, and vapor densities of [EMIM][TFSA] and [BuPY][BF_4] as they are slowly heated from 1000 to 1500 K. Interestingly, the total Lennard-Jones (LJ) contribution in the case of [EMIM][TFSA] is considerably higher than the electrostatic (EL) energy, E_{LJ} = −47.4 kJ mol^{-1}, while E_{EL} = +4.8 kJ mol^{-1} at 1000 K. Thus, attraction between the cation and anion is completely compensated for by cation−cation and

Received: April 3, 2012
Accepted: June 4, 2012
Published: June 4, 2012

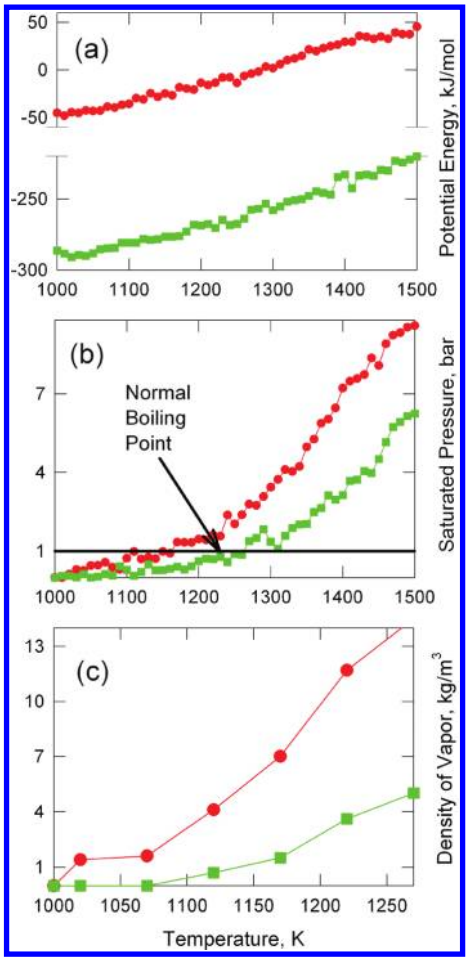

Figure 1. (a) Energy evolution in the RTIL systems upon heating; (b) saturated vapor pressure evolution; (c) liquid state specific density evolution of [EMIM][TFSA] (red circles) and [BuPY][BF_4] (green squares).

anion−anion repulsion. Contrariwise, electrostatic attraction is more than 10 times higher for [BuPY][BF_4] at the same temperature. Consequently, the saturated vapor pressure (Figure 1b) of [BuPY][BF_4] is smaller and the normal boiling temperature is higher (1230 versus 1150 K). Both RTILs exhibit similar average vapor-phase densities (Figure 1c) at their respective boiling points (~4 kg m^{-3}), which are comparable with those of molecular liquids.

In the context of our investigation, it may be useful to demonstrate that the temperatures of liquid and vapor phases are similar during simulation. Figure S1 (Supporting Information) plots the temperature of the vapor subsystem of [BuPY][BF_4] at 1050 K (thermostat *T*) while using velocity rescaling and Berendsen thermostats with the 250 fs response time in both cases. We observe no temperature drift during 1000 ps of simulation. The average vapor temperature equals 1049.2 K with the velocity rescaling thermostat. The data indicate that the two phases creating the interface are maintained at similar temperatures.

Figure 2 depicts the temperature-depended evolution of the liquid and vapor phases, while Figure 3 demonstrates our determination of the critical points. The results are in total agreement with the energies and pressures discussed above. In this study, we define the liquid phase as a cluster of maximum size at any given moment of time, provided that it does not lose

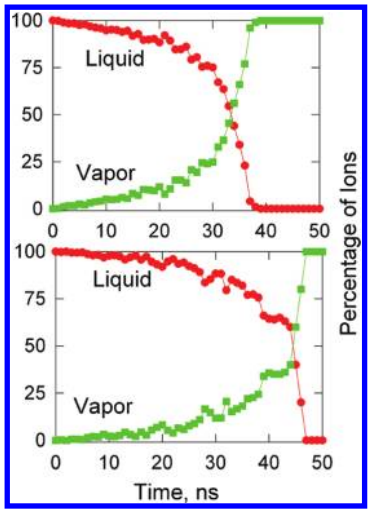

Figure 2. The percentages of liquid and gaseous phases versus simulation time of [EMIM][TFSA] (top) and [BuPY][BF_4] (bottom).

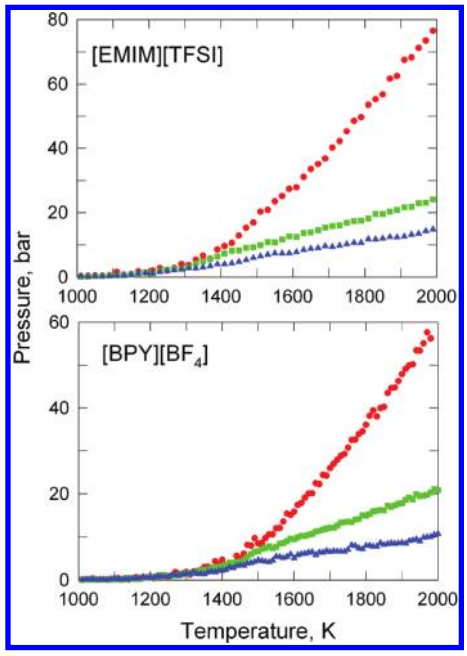

Figure 3. Critical point determination: vapor pressure increase upon heating of the MD systems of different volumes, 65.1 × 65.1 × 750 Å (red circles), 65.1 × 65.1 × 1000 Å (green squares), and 65.1 × 65.1 × 1250 Å (blue triangles).

more than 10% of the particles during the latest 10 ps of the trajectory. All ions that do not belong to the liquid phase defined above belong to the vapor. The algorithm applied to split the simulated system into clusters is described in the Methodology section. As numerically illustrated below, such a definition provides a reliable way to distinguish between vapor and liquid phases upon heating. While almost 100% of the simulated ions exist as liquid at 1000 K, the situation drastically changes after the 20th nanosecond (corresponding to 1200 k). Eventually, all ions transfer from the liquid to the vapor phase at critical points, which are 1340 and 1460 K for [EMIM]-[TFSA] and [BuPY][BF_4], respectively.

In addition to assigning the critical points on the basis of the liquid/vapor coexistence, they are identified independently, as illustrated in Figure 3. The RTIL bulk system is expanded along

dx.doi.org/10.1021/jz300405q | *J. Phys. Chem. Lett.* 2012, 3, 1657−1662

one of the axes to create three systems, so that the expanded sides are 750, 1000, and 1250 Å long, whereas the two remaining box sides are not changed (65.1 Å). Above the critical point, the system cannot be condensed and occupies uniformly all available volume. The pressure is inversely proportional to the volume. Because the three systems have different volumes, the same pressure is observed below the critical point, but the pressures differ upon further heating. Indeed, Figure 3 demonstrates that the lines for [EMIM][TFSA] and [BuPY][BF_4] diverge at ~1340 and ~1460 K, which are in excellent agreement with the conclusions of Figure 2. Both boiling and critical points of the considered imidazolium- and pyridinium-based RTILs are much higher than those of any molecular liquid. As indicated by the high boiling and critical points, interionic interactions are very strong, suggesting that ionic vapor can create surprising structures, likely more complicated than isolated ions and/or ion pairs.

The rate of heating (1 K/100 ps) may intuitively seem quite fast to maintain the quasi-equilibrium regime. In particular, the 100 ps time should be enough to re-equilibrate the interface as the temperature increases by 1 K. This time has to be longer than the characteristic time for formation and re-formation of vaporized ionic clusters. To address this issue, we monitor the interionic interaction energy during the nonequilibrium MD simulation (Figure S2, Supporting Information) starting with the liquid/vacuum interface (i.e., no vapor). While the energy relaxation time generally depends on the temperature of the liquid phase, in no case of our study does it exceed 30 ps. We conclude that heating of 1 K per 100 ps is safe to allow for continuous evolution of the liquid/vapor system structure from 1000 to 2000 K.

Pressure is a macroscopic property, which is often poorly defined for nanoscale and even mesoscale systems because of large fluctuations. Either a very long time, Δt, or a very large simulation box is required to obtain converged pressure values. To reduce the fluctuations, we provide the vapor phase with a volume of ~4000 nm^3. Figure S3 (Supporting Information) investigates whether temperature ramping at the rate of 1K per 100 ps is sufficiently slow to get reliable average pressures (Figure 3). The standard errors (estimated using several independent MD runs) depend on the temperature more strongly than on the length of the trajectory used for each temperature. The estimated errors for the 100 ps interval are 29, 10, and 4% at 1100, 1300, and 1700 K, respectively. If accurate pressure values are desirable at $T \approx 1000$ K, trajectories much longer than 100 ps should be used (see Figure S3, Supporting Information). Note that in Figure 3, the temperature changes in 5 K steps to provide smooth pressure curves.

Cluster analysis of the ionic vapor is reported at several temperatures between 1000 and 1100 K (Figures 4 and 5). Although it may be interesting to provide such an analysis above the normal boiling point as well, we suppose that the corresponding ionic formations are unstable and depend strongly on the vapor density/pressure. In this work, we concentrate the efforts on the composition of RTIL vapor only below the boiling point.

As can be expected, the most probable ionic formation in vapor is the ion pair. More than half of all vaporized ions exist in this form at 1000 K. Interestingly, the amount of neutral ion pairs of [BuPY][BF_4] significantly decreases with increasing temperature (Figure 5), whereas it does not change for

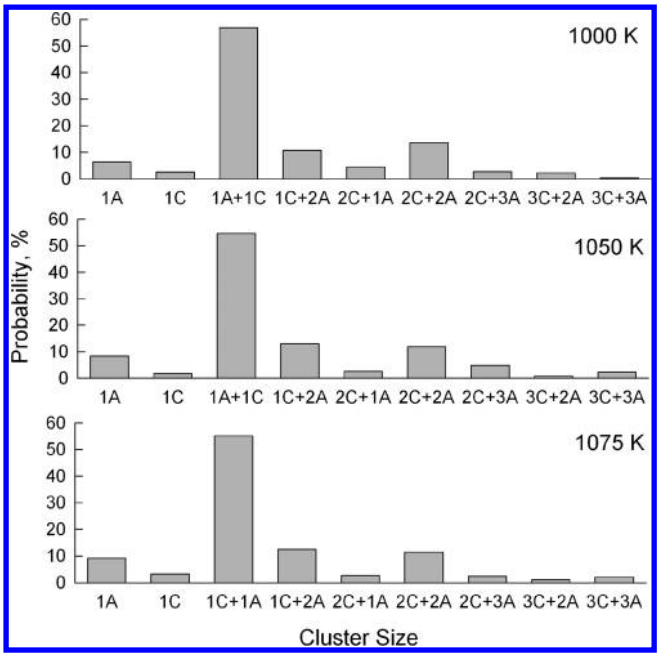

Figure 4. The ionic formations observed in the saturated vapor phase of [EMIM][TFSA]. The composition of each species is designated as nC + mA, where C is a cation, A is an anion, and n and m are their respective quantities in a cluster.

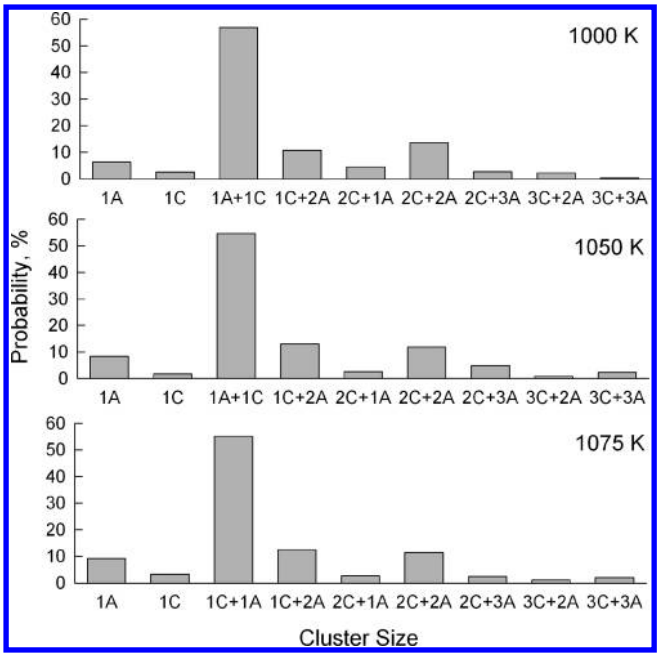

Figure 5. The ionic formations observed in the saturated vapor phase of [BuPY][BF_4]. The notation is the same as in Figure 4.

[EMIM][TFSA] (Figure 4). Our observation is supported by the recently published experiment of Armstrong et al.,[20] who employed the line-of-sight mass spectrometry. The measurements were carried out on thermally evaporated [EMIM][TFSA] and several other imidazolium-based RTILs in a temperature-programmed desorption run at 522 K. Only peaks corresponding to cations are detected in the spectra, indicating that the initial vapor consists exclusively of ion pairs, according to the following mechanism. Electron bombardment knocks off an electron from the $[TFSA]^-$ anion and transforms the latter

dx.doi.org/10.1021/jz300405q | J. Phys. Chem. Lett. 2012, 3, 1657−1662

into a neutral radical. Subsequently, the ionic bond keeping the ion pair together breaks, and the cation is accelerated within the quadrupole field toward the counter. While the procedure cannot detect anions, it determines well the positively charged products of the ion pair decomposition. Similar conclusions about ion pair stability have been reported recently on the basis of time-of-flight secondary ion mass spectrometry in vacuum[22] and atmospheric pressure chemical ionization mass spectrometry.[21]

Upon reducing the emission current in the mass spectrometer, the intensity of the cation peak decreases proportionally, and upon reducing the electron bombardment ionization energy to zero, the cation peak vanishes. Thus, it is argued that the signal originates exclusively from the artificial ionization of the vapor phase, while no free cations (and therefore, anions) exist in imidazolium-based RTILs.[20] Our simulation shows that $[EMIM]^+$ does exists in the pristine vapor, although its content is less than 3%. The content of $[TFSA]^-$ ranges between 7 and 9%. The inequality of the cation and anion fractions in the vapor is compensated for by larger charged formations. The existence of a non-negligible percentage of charged species is reported in the previous computational studies using all-atom empirical potential models for 1-butyl-3-methylimidazolium triflate[25] and a series of 1-alkyl-3-methylimidazolium tetrafluoroborates.[19] The latter work considers saturated vapor of RTILs at 900−1100 K, that is, the same temperature range as that in our investigation. A small population of non-neutral species (∼2%) is also observed for alkylimidazolium TFSA ionic liquids.[23]

The mass spectrometry results contain no peaks corresponding to charged clusters of the form $[EMIM]_n[TFSA]_m^+$, where n and m are positive integers. Therefore, it is concluded that vaporized ion clusters are unstable and that the corresponding ionized species are fragmented into individual cations and neutral radicals. Note that the clusters with $m = 1$ are destroyed by the electron bombardment. It remains unclear whether clusters with $m > 1$ are accessible experimentally using the above technique. Our simulation shows that the investigated vapor consists of a variety of clusters, some of which are as large as $[EMIM]_3[TFSA]_3$ and $[BUPY]_3[BF_4]_3$. No larger formations are observed even with negligible probabilities during 50 000 ps of the simulation. Negative clusters are more stable than positive ones in the case of [EMIM][TFSA]. The situation is completely reversed in the case of $[BuPY][BF_4]$. Nearly no free BF_4^- anions are found at any temperature between 1000 and 1100 K. This is most likely due to the large partial charges on the fluorine atoms (i.e., polar B−F bonds).[9] Even if $[BF_4]^-$ evaporates as a free particle, it quickly finds a cation (or two cations; see Figure 5) and creates a stable cluster.

Remarkably, although $[EMIM]^+$ and $[BuPY]^+$ are similar in some aspects of chemical structure, for example, both (1) consist of carbons, hydrogens, and nitrogens only, (2) contain heterocyclic aromatic rings that accommodate most of the positive charge, and (3) possess inert alkyl tails, they exhibit very different cluster size distributions. First, the probability of ion pair formation is independent of temperature in the case of [EMIM][TFSA], but it decreases almost two times when $[BuPY][BF_4]$ is heated from 1000 to 1100 K. Second, $[BuPY][BF_4]$ tends to create charged clusters more readily than [EMIM][TFSA]. Currently, we are not aware of experimental studies of the $[BuPY][BF_4]$ vapor to compare the simulation results. Third, the large five-ion clusters contribute more than 10% to the $[BuPY][BF_4]$ vapor, whereas they are marginal in [EMIM][TFSA]. The average size of the ion cluster increases in both RTILs with growing temperature. On the one hand, a higher temperature provides more kinetic energy that can break ionic bonds. On the other hand, it facilitates evaporation, increasing the vapor density (Figure 1c) and, therefore, favoring larger clusters.

The RTIL films used in this study are comparatively small, containing 500 ion pairs. One can expect that the accuracy of liquid-phase representation can influence the cluster distributions. In order to test the role of the system size, much larger systems, containing 10 000 and 25 000 ion pairs of $[BuPY][BF_4]$ (290 000 and 725 000 interaction centers) in boxes of 10^6 and 10^7 nm^3 volumes are used to derive the cluster distributions at 1050 K (Figure S4, Supporting Information). No correlations are found between the number of atoms in the film and the composition of the ionic clusters in the vapor. Therefore, we conclude that at $T = 1050$ K RTILs exhibit little long-range structure and generally resemble molecular liquids. Thus, the liquid/vapor interface can be implemented realistically using systems of as small as 500 ion pairs.

To recapitulate, the available experiments suggest that RTIL vapor consists exclusively of neutral ion pairs. Our simulations show that it also contains a wide variety of relatively complex species and that the fraction of charged clusters is non-negligible. This difference between the physical and numerical experiments can be explained by the fact that mass spectrometry applies thermal evaporation at a relatively low temperature (e.g., 522 K[20]), while our simulation describes spontaneous vaporization above 1000 K. It is likely that at lower temperatures, the ions lack the kinetic energy needed to break the ionic bond of the neutral pair. By performing the first molecular dynamics simulation of its kind, we demonstrate that free anions exist in saturated vapor of RTILs. Detection of these species presents a challenge to mass spectrometry. Quite surprisingly, clusters with three cations and three anions do exist between 1000 and 1100 K. We expect that even larger clusters will be found at higher temperatures and pressures/vapor densities, as recently shown by Maginn et al.[23] These conclusions are particularly important for RTIL applications that rely on the RTIL ability to solvate chemical compounds.

METHODOLOGY

The reported results are obtained using atomistic equilibrium and nonequilibrium MD simulations. Nonequilibrium MD mimics real-time behavior of RTILs upon heating (Figures 1−3). Equilibrium MD is used to sample ion formations (Figures 4 and 5) in the RTIL vapor in equilibrium with a RTIL. Each simulated sample of [EMIM][TFSA] and $[BuPY][BF_4]$ contains 500 ion pairs.

First, the systems are equilibrated as periodic liquids at 1000 K in the constant pressure/constant temperature ensemble to achieve the corresponding density. Second, the liquid/vapor interface is created by elongating the system along one of the Cartesian directions. Third, the systems are heated with the rate of 1 K per 100 ps to ensure a quasi-equilibrium regime. This stage is performed in the constant volume/constant temperature ensemble. Fourth, the heating is stopped at 1000, 1050, 1075, and 1110 K, and the systems are additionally relaxed. The 50 000 ps equilibrium trajectories are generated, and atomic coordinates are saved every 2 ps for subsequent cluster analysis. During these simulation stages, the velocity rescaling thermostat[36] and the Parrinello−Rahman barostat[37] (where applicable) with relaxation times of 0.5 and 4 ps, respectively, are

dx.doi.org/10.1021/jz300405q | J. Phys. Chem. Lett. 2012, 3, 1657−1662

employed to maintain a requested temperature and the 1 bar pressure. The electrostatic interactions are computed using the reaction-field-zero scheme[38] with the 1.5 nm cutoff radius. The shifted force method is used to gradually decrease the LJ potential to zero at 1.3 nm. The equations of motion are integrated with the 0.001 ps time step. All bonds involving hydrogen atoms are kept rigid using the SHAKE algorithm. Test simulations indicate that freezing the C−H bond length does not influence the macroscopic properties in any systematic way; meanwhile, it improves the stability of the MD algorithms at high temperatures. The FF models of $[EMIM]^+$, $[BUPY]^+$, $[TFSA]^-$, and BF_4^- are obtained from the Canongia Lopes and Padua's parameters published elsewhere.[35] These parameters are generated using a well-defined procedure that can be extended to other systems. Although this set of parameters does not account for electronic polarization in the condensed phase[39] and consequently provides systematically overestimated heats of vaporization, for example, H_{vap}([EMIM][TFSA]) = 162 kJ mol^{-1} (simulated) and H_{vap}([EMIM][TFSA]) = 134 kJ mol^{-1} (experimental), at 298 K and 1 bar, the polarization effect greatly decreases as the temperature increases.[40] In this simulation study, we assume that polarization is negligible in liquid and vaporized RTILs above 1000 K.

The cluster analysis of the RTIL vapor phase is performed as follows. Two structures are assumed to form a cluster if they exhibit at least one direct contact. A third structure belongs to this cluster if it possesses at least one direct contact with any atom of the first two structures, and so on. The analysis continues iteratively at each trajectory frame until all structures are exhausted.

All molecular dynamics trajectories are generated using the GROMACS package.[38,41] The analysis of the results is carried out by homemade programs (developed by V.V.C.) and GROMACS auxiliary utilities where possible. The simulations are carried out in parallel using 24−128 processors. A particle decomposition scheme is implemented to distribute particles among nodes.

■ ASSOCIATED CONTENT

Supporting Information

Figures S1−S4. This material is available free of charge via the Internet at http://pubs.acs.org.

■ AUTHOR INFORMATION

Corresponding Author

*Tel. +1-585-276-5751. E-mail: vvchaban@gmail.com; v.chaban@rochester.edu.

Notes

The authors declare no competing financial interest.

■ ACKNOWLEDGMENTS

The research is supported by the NSF Grant CHE-1050405.

■ REFERENCES

(1) Earle, M. J.; Esperanca, J. M. S. S.; Gilea, M. A.; Lopes, J. N. C.; Rebelo, L. P. N.; Magee, J. W.; Seddon, K. R.; Widegren, J. A. The Distillation and Volatility of Ionic Liquids. *Nature* **2006**, *439*, 831−834.

(2) Esperanca, J. M. S. S.; Lopes, J. N. C.; Tariq, M.; Santos, L. M. N. B. F.; Magee, J. W.; Rebelo, L. P. N. Volatility of Aprotic Ionic Liquids — A Review. *J. Chem. Eng. Data* **2010**, *55*, 3−12.

(3) Spohr, H. V.; Patey, G. N. Structural and Dynamical Properties of Ionic Liquids: The Influence of Ion Size Disparity. *J. Chem. Phys.* **2008**, *129*, 064517.

(4) Wasserscheid, P. Chemistry — Volatile Times for Ionic Liquids. *Nature* **2006**, *439*, 797−797.

(5) Wishart, J. F.; Castner, E. W. The Physical Chemistry of Ionic Liquids. *J. Phys. Chem. B* **2007**, *111*, 4639−4640.

(6) Kobrak, M. N. A Comparative Study of Solvation Dynamics in Room-Temperature Ionic Liquids. *J. Chem. Phys.* **2007**, *127*, 184507.

(7) Chaban, V. Polarizability versus Mobility: Atomistic Force Field for Ionic Liquids. *Phys. Chem. Chem. Phys.* **2011**, *13*, 16055−16062.

(8) Chaban, V. V.; Prezhdo, O. V. A New Force Field Model of 1-Butyl-3-methylimidazolium Tetrafluoroborate Ionic Liquid and Acetonitrile Mixtures. *Phys. Chem. Chem. Phys.* **2011**, *13*, 19345−19354.

(9) Spohr, H. V.; Patey, G. N. Structural and Dynamical Properties of Ionic Liquids: The Influence of Charge Location. *J. Chem. Phys.* **2009**, *130*, 104506.

(10) Castner, E. W.; Funston, A. M.; Fadeeva, T. A.; Wishart, J. F. Fluorescence Probing of Temperature-Dependent Dynamics and Friction in Ionic Liquid Local Environments. *J. Phys. Chem. B* **2007**, *111*, 4963−4977.

(11) Li, H. L.; Ibrahim, M.; Agberemi, I.; Kobrak, M. N. The Relationship between Ionic Structure and Viscosity in Room-Temperature Ionic Liquids. *J. Chem. Phys.* **2008**, *129*, 124507.

(12) Zhao, H.; Malhotra, S. V. Applications of Ionic Liquids in Organic Synthesis. *Aldrichimica Acta* **2002**, *35*, 75−83.

(13) Zhao, D. B.; Wu, M.; Kou, Y.; Min, E. Ionic liquids: Applications in Catalysis. *Catal. Today* **2002**, *74*, 157−189.

(14) Chen, R. J.; Zhang, H. Q.; Wu, F. Applications of Ionic Liquids in Batteries. *Prog. Chem.* **2011**, *23*, 366−373.

(15) Emel'yanenko, V. N.; Verevkin, S. P.; Heintz, A. the Gaseous Enthalpy of Formation of the Ionic Liquid 1-Butyl-3-methylimidazolium Dicyanamide from Combustion Calorimetry, Vapor Pressure Measurements, And Ab Initio Calculations. *J. Am. Chem. Soc.* **2007**, *129*, 3930−3937.

(16) Zaitsau, D. H.; Kabo, G. J.; Strechan, A. A.; Paulechka, Y. U.; Tschersich, A.; Verevkin, S. P.; Heintz, A. Experimental Vapor Pressures of 1-Alkyl-3-methylimidazolium Bis(trifluoromethylsulfonyl) Imides and a Correlation Scheme for Estimation of Vaporization Enthalpies of Ionic Liquids. *J. Phys. Chem. A* **2006**, *110*, 7303−7306.

(17) Taylor, A. W.; Lovelock, K. R. J.; Deyko, A.; Licence, P.; Jones, R. G. High Vacuum Distillation of Ionic Liquids and Separation of Ionic Liquid Mixtures. *Phys. Chem. Chem. Phys.* **2010**, *12*, 1772−1783.

(18) Leal, J. P.; da Piedade, M. E. M.; Lopes, J. N. C.; Tomaszowska, A. A.; Esperanca, J. M. S. S.; Rebelo, L. P. N.; Seddon, K. R. Bridging the Gap between Ionic Liquids and Molten Salts: Group 1 Metal Salts of the Bistriflamide Anion in the Gas Phase. *J. Phys. Chem. B* **2009**, *113*, 3491−3498.

(19) Rai, N.; Maginn, E. J. Vapor−Liquid Coexistence and Critical Behavior of Ionic Liquids via Molecular Simulations. *J. Phys. Chem. Lett.* **2011**, *2*, 1439−1443.

(20) Armstrong, J. P.; Hurst, C.; Jones, R. G.; Licence, P.; Lovelock, K. R. J.; Satterley, C. J.; Villar-Garcia, I. J. Vapourisation of Ionic Liquids. *Phys. Chem. Chem. Phys.* **2007**, *9*, 982−990.

(21) Neto, B. A. D.; Santos, L. S.; Nachtigall, F. M.; Eberlin, M. N.; Dupont, J. On the Species Involved in the Vaporization of Imidazolium Ionic Liquids in a Steam-Distillation-Like Process. *Angew. Chem., Int. Ed.* **2006**, *45*, 7251−7254.

(22) Smith, E. F.; Rutten, F. J. M.; Villar-Garcia, I. J.; Briggs, D.; Licence, P. Ionic Liquids in Vacuo: Analysis of Liquid Surfaces Using Ultra-High-Vacuum Techniques. *Langmuir* **2006**, *22*, 9386−9392.

(23) Rai, N.; Maginn, E. J. Critical Behaviour and Vapour−Liquid Coexistence of 1-Alkyl-3-methylimidazolium Bis(trifluoromethylsulfonyl)amide Ionic Liquids via Monte Carlo Simulations. *Faraday Discuss.* **2012**, *154*, 53−69.

(24) Berg, R. W.; Lopes, J. N. C.; Ferreira, R.; Rebelo, L. P. N.; Seddon, K. R.; Tomaszowska, A. A. Raman Spectroscopic Study of the

Vapor Phase of l-Methylimidazolium Ethanoate, a Protic Ionic Liquid. *J. Phys. Chem. A* **2010**, *114*, 10834−10841.
(25) Ballone, P.; Pinilla, C.; Kohanoff, J.; Del Popolo, M. G. Neutral and Charged 1-Butyl-3-methylimidazolium Triflate Clusters: Equilibrium Concentration in the Vapor Phase and Thermal Properties of Nanometric Droplets. *J. Phys. Chem. B* **2007**, *111*, 4938−4950.
(26) Lovelock, K. R. J.; Deyko, A.; Corfield, J. A.; Gooden, P. N.; Licence, P.; Jones, R. G. Vaporisation of a Dicationic Ionic Liquid. *ChemPhysChem* **2009**, *10*, 337−340.
(27) Deyko, A.; Lovelock, K. R. J.; Licence, P.; Jones, R. G. The Vapour of Imidazolium-Based Ionic Liquids: A Mass Spectrometry Study. *Phys. Chem. Chem. Phys.* **2011**, *13*, 16841−16850.
(28) Lovelock, K. R. J.; Deyko, A.; Licence, P.; Jones, R. G. Vaporisation of an Ionic Liquid near Room Temperature. *Phys. Chem. Chem. Phys.* **2010**, *12*, 8893−8901.
(29) Deyko, A.; Lovelock, K. R. J.; Corfield, J. A.; Taylor, A. W.; Gooden, P. N.; Villar-Garcia, I. J.; Licence, P.; Jones, R. G.; Krasovskiy, V. G.; Chernikova, E. A.; Kustov, L. M. Measuring and Predicting $\Delta H_{vap}(298)$ Values of Ionic Liquids. *Phys. Chem. Chem. Phys.* **2009**, *11*, 8544−8555.
(30) Verevkin, S. P.; Zaitsau, D. H.; Emelyanenko, V. N.; Heintz, A. A New Method for the Determination of Vaporization Enthalpies of Ionic Liquids at Low Temperatures. *J. Phys. Chem. B* **2011**, *115*, 12889−12895.
(31) Preiss, U.; Verevkin, S. P.; Koslowski, T.; Krossing, I. Going Full Circle: Phase-Transition Thermodynamics of Ionic Liquids. *Chem.—Eur. J.* **2011**, *17*, 6508−6517.
(32) Vitorino, J.; Leal, J. P.; da Piedade, M. E. M.; Lopes, J. N. C.; Esperanca, J. M. S. S.; Rebelo, L. P. N. The Nature of Protic Ionic Liquids in the Gas Phase Revisited: Fourier Transform Ion Cyclotron Resonance Mass Spectrometry Study of 1,1,3,3-Tetramethylguanidinium Chloride. *J Phys Chem B* **2010**, *114*, 8905−8909.
(33) Neves, P.; Gago, S.; Balula, S. S.; Lopes, A. D.; Valente, A. A.; Cunha-Silva, L.; Paz, F. A. A.; Pillinger, M.; Rocha, J.; Silva, C. M.; Goncalves, I. S. Synthesis and Catalytic Properties of Molybdenum-(VI) Complexes with Tris(3,5-dimethyl-1-pyrazolyl)methane. *Inorg. Chem.* **2011**, *50*, 3490−3500.
(34) Rocha, M. A. A.; Lima, C. F. R. A. C.; Gomes, L. R.; Schroder, B.; Coutinho, J. A. P.; Marrucho, I. M.; Esperanca, J. M. S. S.; Rebelo, L. P. N.; Shimizu, K.; Lopes, J. N. C.; Santos, L. M. N. B. F. High-Accuracy Vapor Pressure Data of the Extended $[C_nC_1im][Ntf_2]$ Ionic Liquid Series: Trend Changes and Structural Shifts. *J. Phys. Chem. B* **2011**, *115*, 10919−10926.
(35) Lopes, J. N. C.; Padua, A. A. H. Molecular Force Field for Ionic Liquids Iii: Imidazolium, Pyridinium, And Phosphonium Cations; Chloride, Bromide, And Dicyanamide Anions. *J. Phys. Chem. B* **2006**, *110*, 19586−19592.
(36) Bussi, G.; Donadio, D.; Parrinello, M. Canonical Sampling through Velocity Rescaling. *J. Chem. Phys.* **2007**, *126*, 014101.
(37) Parrinello, M.; Rahman, A. Polymorphic Transitions in Single-Crystals — A New Molecular-Dynamics Method. *J. Appl. Phys.* **1981**, *52*, 7182−7190.
(38) Hess, B.; Kutzner, C.; van der Spoel, D.; Lindahl, E. GROMACS 4: Algorithms for Highly Efficient, Load-Balanced, And Scalable Molecular Simulation. *J. Chem. Theory Comput.* **2008**, *4*, 435−447.
(39) Borodin, O. Polarizable Force Field Development and Molecular Dynamics Simulations of Ionic Liquids. *J. Phys. Chem. B* **2009**, *113*, 11463−11478.
(40) Chaban, V. V.; Voroshylova, I. V.; Kalugin, O. N. A New Force Field Model for the Simulation of Transport Properties of Imidazolium-Based Ionic Liquids. *Phys. Chem. Chem. Phys.* **2011**, *13*, 7910−7920.
(41) Berendsen, H. J. C.; Van der Spoel, D.; Lindahl, E.; Hess, B.; Groenhof, G.; Mark, A. E. GROMACS: Fast, Flexible, And Free. *J. Comput. Chem.* **2005**, *26*, 1701−1718.